

# EVN and MERLIN Observations of the FR 1 Radio Galaxy 3C 264

L. Lara <sup>a,b,1</sup>, G. Giovannini <sup>a,c</sup>, W.D. Cotton <sup>d</sup>, L. Feretti <sup>a</sup>,  
T. Venturi <sup>a</sup>, S.A. Baum <sup>e</sup>, C.P. O’Dea <sup>e</sup>,  
S. de Koff <sup>e,f</sup> and W.B. Sparks <sup>e</sup>

<sup>a</sup>*Istituto di Radioastronomia, Via Gobetti 101, 40129 Bologna, Italy*

<sup>b</sup>*Instituto de Astrofísica de Andalucía, CSIC, Apdo. 3004, 18080 Granada, Spain*

<sup>c</sup>*Dipartimento di Astronomia, Università di Bologna, Italy*

<sup>d</sup>*NRAO, 520 Edgemont Road, Charlottesville, VA 22903-2475, USA*

<sup>e</sup>*STScI, 3700 San Martin Drive, Baltimore, MD 21218, USA*

<sup>f</sup>*Sterrewacht, Leiden, The Netherlands*

We present results from simultaneous EVN and MERLIN observations of the FR 1 radio galaxy 3C 264 at 5 GHz. The combination of these two arrays allows us to obtain radio images with resolutions ranging from 4.6 to 118 mas. Moreover, we compare similar resolution images from MERLIN and the HST, compute the spectral index along the jet between optical and radio wavelengths, and confirm the synchrotron nature of the optical jet in 3C 264.

## 1 The Radio Galaxy 3C 264

3C 264 (B 1142+198) is a low luminosity radio source identified with NGC 3862 [ $m_v = 13.67$ ;  $z = 0.0206$ ], a bright galaxy in the Abell cluster 1367. NGC 3862 contains a compact ( $\sim 2$  arcsec) and possibly variable X-ray source embedded in the diffuse X-ray emission from the intra-cluster medium, in a position consistent with that of the central 5 GHz radio source component [4]. NGC 3862 also contains an oval region of line-emitting gas of  $\sim 6.3$  arcsec in extent, centered on the galaxy nucleus, with its major axis roughly perpendicular to the radio source ejection axis [1]. A bright optical jet, with a length of  $\sim 0.65$  arcsec, was discovered with the Hubble Space Telescope (HST) [3].

---

<sup>1</sup> The author wishes to acknowledge support for this research by the European Union under contract CHGECT920011.

The radio structure of 3C 264 presents, at arc-second scales, a head-tailed morphology [5], with a prominent core and a wiggled jet extending toward the northeast. The magnetic field appears parallel to the jet axis in the proximity of the core, becoming perpendicular at an angular distance of  $\sim 3$  arcsec. The flux density of the VLA core is  $\sim 260$  mJy. Flux density variability of the core has not been reported in the literature. There is some evidence of a counter-jet extending southwest from the core [6]. The jet and counter-jet are embedded in a very extended and diffuse emission that fades to the noise level and seems to be dragged along the north. The maximum angular size of 3C 264 is  $9'$  [5].

## 2 Observations and Data Reduction

3C 264 was observed simultaneously with the European VLBI Network (EVN) and MERLIN on May 22nd 1995 at a frequency of 5.0 GHz in left circular polarization (LCP). The observing bandwidth was 28 MHz for the EVN and 16 MHz for MERLIN.

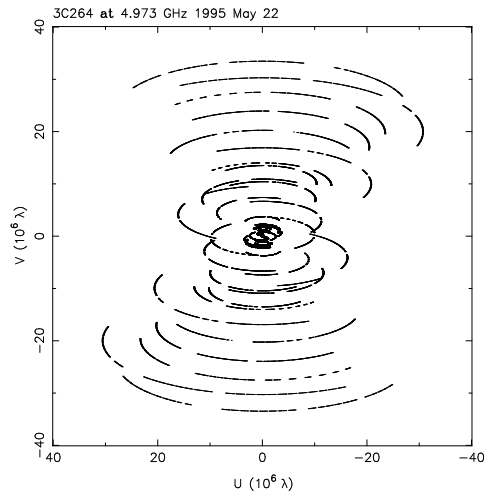


Fig. 1.  $uv$ -coverage of the combined EVN + MERLIN data

The EVN array consisted of 7 antennas: Effelsberg, Cambridge, Jodrell-MK2, Medicina, Noto, Onsala and Westerbork. The EVN data were correlated at the MPIfR (Bonn), and later fringe-fitted using the NRAO AIPS package. The data were initially calibrated using the measured system temperatures and antenna gains.

The MERLIN array consisted of six antennas: Tabley, Cambridge, Jodrell-MK2, Darnhall, Knockin and Defford. Flux density calibration was performed with the OLAF package by comparison of OQ208 and 1144+402 with the flux density calibrator 3C286.

We used the `Difmap` and the `AIPS` packages for imaging the EVN and the MERLIN data, respectively, following standard self-calibration and mapping procedures. Once the separate maps from each array were produced, we proceeded to combine the self-calibrated EVN and MERLIN data. Fig. 1 shows the  $uv$  coverage of the combined data. Since different calibration schemes were applied to each data set, the relative flux density scales were misaligned and had to be adjusted. We used the EVN image as the initial source model in the mapping procedure.

In Fig. 2 we present maps of 3C 264 at 5.0 GHz obtained with the EVN, MERLIN and combination of these two arrays, ordered in decreasing angular resolution, from 4.6 mas to 118 mas (geometric mean of HPBW). To obtain these maps, we used the `Difmap` package, selecting cleaning boxes with more external jet regions in each hybrid mapping iteration, and changing the data weighting by applying progressively stronger Gaussian  $uv$ -tapers to the data. In this way, we finally obtained a unique model which describes the visibility data in all  $uv$ -spacings.

### 3 Observational Results

At 4.6 mas resolution (Fig.2a), we observe a compact core component from which a smooth jet emerges with a position angle (P.A.) of  $26^\circ$ . At this resolution it is difficult to discriminate any well defined component in the jet, and hence to study the possibility of superluminal motion in 3C 264. A similar structure was found in previous global VLBI observations [6]. However, with slightly lower resolution (7.9 mas, Fig.2b), a component which is only slightly indicated in the EVN map appears clearly at a distance of  $\sim 53$  mas from the core. At still lower resolution (Fig.2c-e), we observe a well collimated jet with a small opening angle, which, at a distance of 0.25 arcsec changes its properties increasing the opening angle and the wiggle amplitude in a way that suggests a helical structure (Fig.2c). The average P.A. of the jet at these scales is  $37^\circ$ . At a distance of 0.77 arcsec from the core we observe a re-collimation of the jet, and further on, at 1.4 arcsec, a remarkable fall in the surface brightness (Fig.2f).

### 4 Comparison of Optical and Radio Images

A recent HST optical continuum WFPC2 image of 3C 264 confirms the existence of an optical jet extending for  $\sim 2.2$  arcsec [2]. Since the HST and MERLIN provide similar angular resolution, we have obtained the spectral index map between the optical and the radio wavelengths. We transformed

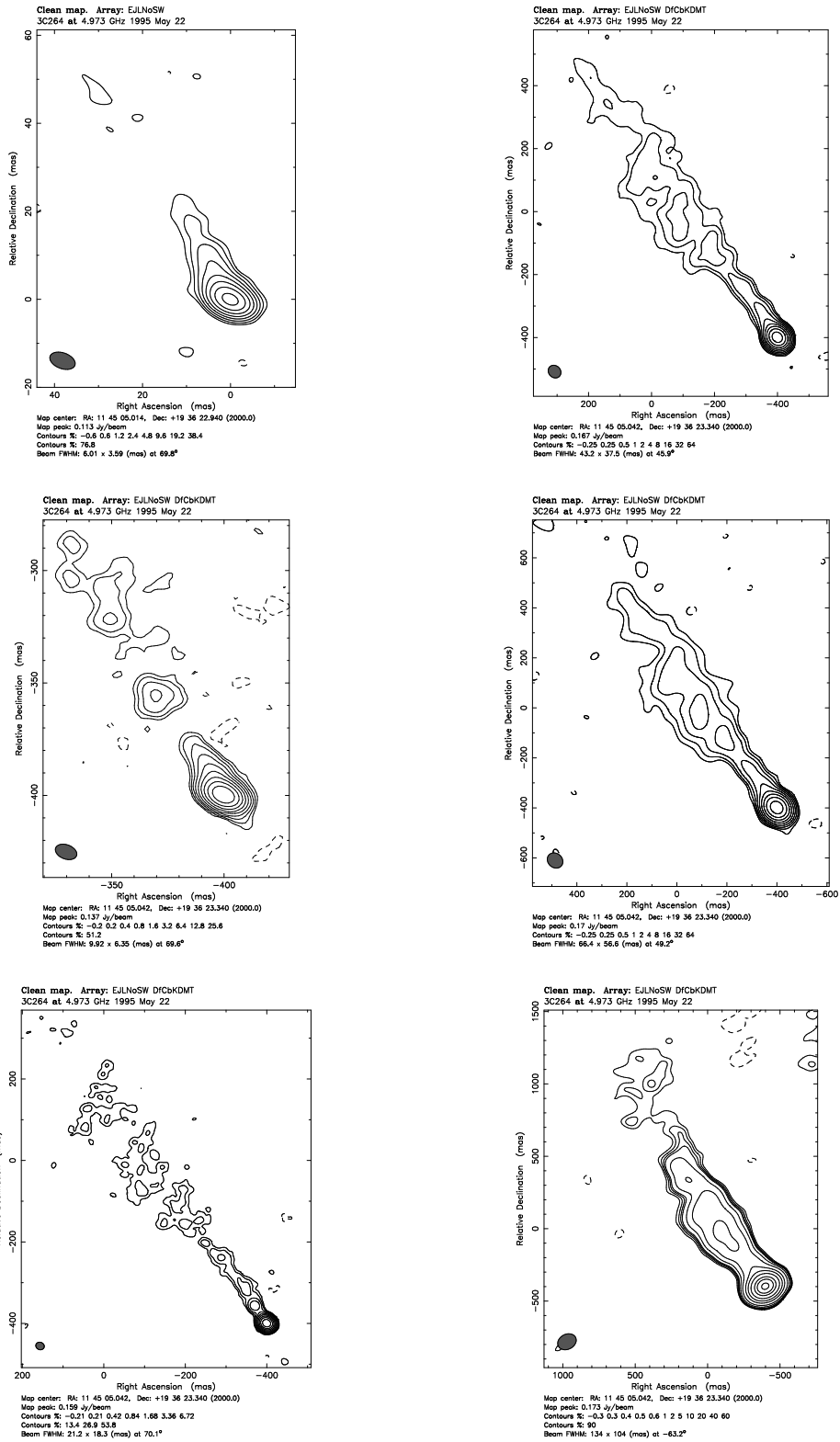


Fig. 2. a-f. From top to bottom and left to right, EVN and MERLIN images of 3C 264 at 5 GHz ordered in decreasing angular resolution

the MERLIN image, so that it had the same pixel size as the HST image (45 mas), and then registered both images by the peak of brightness of the core. Fig. 3a shows the overlay of a contour plot of the WFPC2 image on the MER-

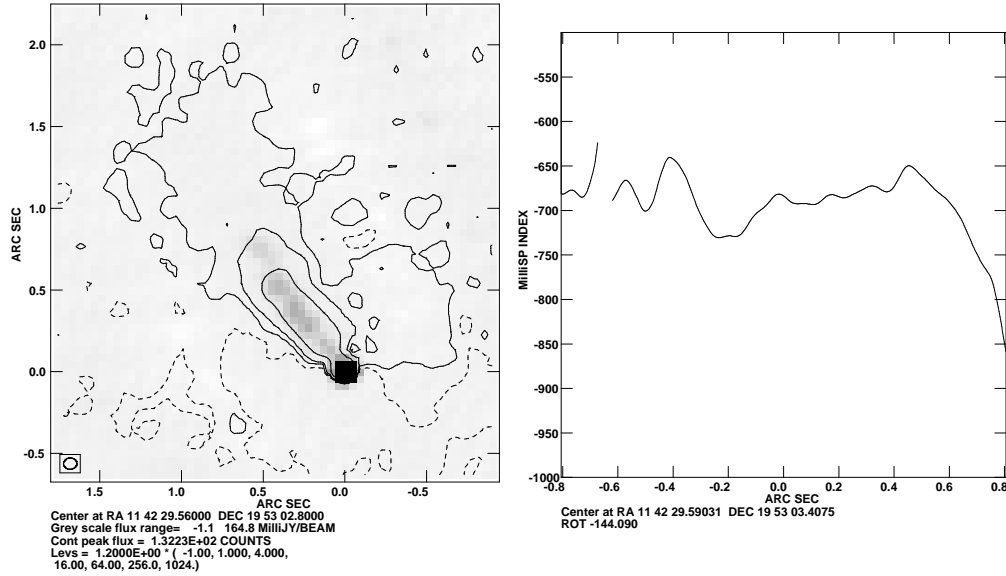


Fig. 3. a.- Overlay of HST (contour plot) and MERLIN (greyscale) images of 3C 264; b.- Slice of the spectral index along the jet (the core is on the right)

LIN image at 5.0 GHz. We find a good correspondence between the spatial distribution of the radio and the optical emissions. Fig. 3b shows a slice of the spectral index along the jet. The spectral index may be affected by the galaxy model subtracted to enhance the jet in the optical image. That could explain the steeper spectrum in the proximity of the core. At further distances along the jet we observe that the spectral index is roughly constant, with a mean value of  $\alpha \sim -0.7$  ( $S \propto \nu^\alpha$ ). In conclusion, the good correspondence between the radio and optical emission, and the value of the jet spectral index confirms the synchrotron nature of the optical jet in 3C 264.

## References

- [1] Baum S. et al., (1988) *Ap. J. S.* **68**, 643.
- [2] Baum S. et al., (1996) *Ap. J.*, in press.
- [3] Crane P. et al., (1993) *Ap. J.* **402**, L37.
- [4] Elvis M. et al., (1981) *Ap. J.* **246**, 20.
- [5] Gavazzi G., Perola C.G., Jaffe W., (1981) *A&A* **103**, 35.
- [6] Lara L. et al., (1997) *Ap. J.* **474**, in press.